Journal of Physical Chemistry and Functional Materials (JPCFM)

journal homepage: http://dergipark.gov.tr/jphcfum

Received: August 5 Accepted: 25 October 2018 Research Article

Determination of The Chemical Effect in The Lanthanide Group of Elements Using Wave Dispersive X-Ray Spectrometry

Sevil (Porikli) Durdağı*, Aslıhan Taşpolat

**Erzincan Binali Yıldırım University, Faculty of Arts and Sciences, Department of Physics, Erzincan, Turkey*

**Corresponding Author: sporikli@gmail.com*

Abstract

In this study, chemical effect changes on the lines of $L_{\alpha 1}$, $L_{\alpha 2}$, $L_{\beta 1}$, $L_{\beta 2}$, $L_{\beta 3}$, $L_{\beta 4}$, $L_{\beta 6}$, $L_{\gamma 1}$, $L_{\gamma 2}$ and $L_{\gamma 3}$ were examined by using a Rigaku single-crystal (LiF) ZSX 100e wavelength dispersive X-Ray spectrometer (WDXRF). In our research, proportional counter (PC) was used for wavelengths less than 0,336 nm and scintillation counter (SC) was used for wavelengths more than 0,154 nm. X-rays could be counted simultaneously both PC and SC in LiF crystal of our device. Depending on the chemical state of the mater, chemical effect may bring about some modifications in values of energy of X-Ray line, full width at half maximum (FWHM), asymmetry index (AI). These effects are different for each main group elements have been investigated to what or what could be caused these differences. Also chemical effects researched depend on status of the chemical bonds and number of valence electrons. Results of the measurements evaluated by Orjin 8.0 program and in order to prevent from faults may occur during the measurements, best experimental geometry conditions determined.

Key Words: WDXRF, X-Ray line, Full width at half maximum (FWHM), Asymmetry index (AI).

1. Introduction

X-ray Fluorescence (XRF) Spectroscopy involves measuring the intensity of X-rays emitted from a specimen as a function of energy or wavelength. Energy Dispersive XRF excites a sample through an X-ray source or radioactive material and collects the resulting excess energy through a detector tube. Wavelength Dispersive XRF also excites a source through an X-ray tube and collects energies with a detector tube. The difference in a WDXRF system is that a crystal between the tubes diffracts X-rays of a specific wavelength into the detector tube; this means that WDXRF can only read X-rays of a single wavelength (and element).

The principal difference between ED and WDXRF techniques lies in the achievable energy (spectral) resolution. WDXRF systems can routinely provide working resolutions between 5 eV and 20 eV, depending on their set up, whereas EDXRF systems typically provide resolutions ranging from 150 eV to 300 eV or more, depending on the type of detector used. The higher resolution of WDXRF provides advantages in reduced spectral overlaps, so that complex samples can be more accurately characterized. Both technologies are equally strong in eliminating background radiation which can affect detection limits and repeatability. WDXRF has a natural advantage due to the high detector resolution but with filters and targets EDXRF can reduce background intensities to provide accurate and repeatable results that are comparable with WDXRF.

X-ray fluorescence spectroscopy has widely been used for elemental analysis and for studying the electronic structure and its relation with the chemical environment [1-3]. With the development of high-resolution X-ray spectrometer, XRF has become a powerful tool to characterize elemental composition and chemical environment in molecules and solids [4,5].

In recent years, chemical state analyses become more interesting topic for many researchers working in the spectroscopy field. Chemical effects on X-ray emissions can be employed for chemical state analysis or characterization of materials [6,7]. Some earlier reports [8] examined the chemical state of F in $xHoF_3$-$20BaF_2$-$10AlF_3$-(70-x) GeO_2 glass using WDXRF spectrometer (45 kV-95 mA) and mentioned that chemical state of fluorine in glass is quite different from HoF_3, BaF_2 and AlF_3compounds. Kainth et al. [9] studied the chemical effect in Ll and Lη XRF spectra of $_{48}$Cd and $_{50}$Sn compounds using WDXRF spectrometer.

In a number of X-ray spectral studies of 3d transition metals it has been observed that the $K\beta$ to $K\alpha$ x-ray intensity ratios are dependent on the physical and chemical environments of the elements in the sample. In the earlier studies of 3d metal compounds [10,12] the influence of the chemical effects has shown difference in the $K\beta$ to $K\alpha$ X-ray intensity ratios up to nearly 10%. Such chemical effects can be caused either by varying 3d electron populations by the admixture of p states from the ligand atoms to the 3d states of the metal or both. In the present work, the fluorescent $L_{\alpha 1}$, $L_{\alpha 2}$, $L_{\beta 1}$, $L_{\beta 2}$, $L_{\beta 3}$, $L_{\beta 4}$, $L_{\beta 6}$, $L_{\gamma 1}$, $L_{\gamma 2}$ and $L_{\gamma 3}$ X-ray spectra of Lanthanum and Cerium in different chemical forms (La, $La_2(CO_3)_3.8H_2O$, $La_2(C_2O_4)_3.10H_2O$, $LaCl_3$, La_2O_3, $La_2(SO_4)_3.9H_2O$, LaF_3, Ce, CeF_3, $Ce_2(SO_4)_3\cdot 8H_2O$, CeH_4, Ce_2O_4, $Ce(SO_4)_2\cdot 4H_2O$ and $Ce_2(CO_3)_3\cdot 5H_2O$) have been measured with high resolution WDXRF spectrometer (Rigaku single-crystal (LiF) ZSX 100e). The positive and negative shifts were measured. Moreover, characteristic quantities such as positions of line maxim, line widths, indices of asymmetry, etc. are determined. These careful measurements show that position of line maxim and the full width at half maximum (FWHM) depend on the chemical form of the element.

2. Experımental Detaıls

The principle of WDXRF spectrometry is the use of different analyzer crystals to diffract and separate the different characteristic wavelengths of the elements present in the sample. Energy resolution and efficiency for each analytical line also depend on the collimator aperture and the analyzer crystal in use. Several different collimators can be used to reduce the step/scan resolution, as well as up to eight analyzer crystals, to better enhance spectral data for a specific element. The crystal analyzer was a place LiF1 (200) crystal (Fig. 1).

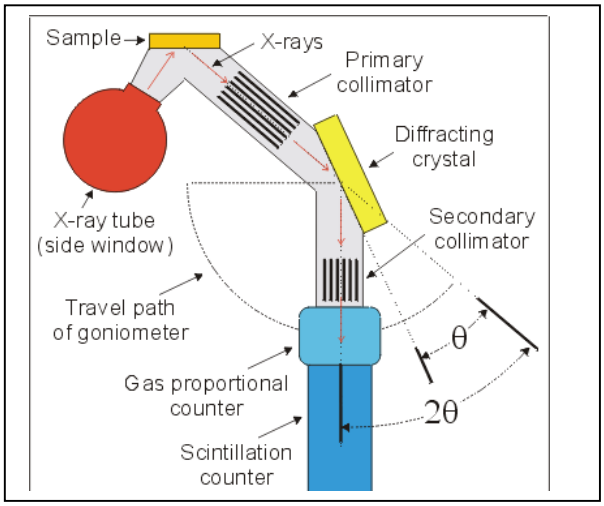

Fig. 1. Experimental Geometry.

The measurements were made with X-ray fluorescence commercial equipment (Rigaku ZSX-100e) with a wavelength dispersive analysis system. This instrument is usually equipped with a 3 kW Rh-anode tube working at a voltage range of 20–50 kV and a current from 50 to 20 mA. It is possible to use primary beam filters (made of Al or Cu) between the primary radiation and the sample holder to reduce the background continuum and to improve the signal-to-noise ratio. Detection can be performed using a flow proportional counter (light elements) or a scintillation counter (heavy elements).

In this work, analyses were made in vacuum atmosphere. X-ray emission spectra were recorded on a fluorescence spectrometer comprising a wide-angle horizontal goniometer by stepping the spectrometer through Bragg angle 2θ in steps of 0.001°. The counting time during the step scanning was selected in such a way that the standard deviation in intensity measurement never exceeded 1%. The dwell time for one channel was defined in such a way that the peak intensity was more than 10 000 counts.

Rigaku has improved their semi-quantitative software package further with the introduction of SQX. It is capable of automatically correcting for all matrix effects, including line overlaps. SQX can also correct for secondary excitation effect by photoelectrons (light and ultra-light elements), varying atmospheres, impurities and different sample sizes. The obtained spectra were converted to energies by inversion of the channels to be treated using the means of the SQX software.

In addition, all of the spectra were plotted by computer in order to reduce subjective and statistical bias. The obtained spectra were analyzed by using the Orgin 8.0 software code to perform spectral deconvolution and fitting and to evaluate element net peak areas from the spectra. Peak fitting was done by iteration to better adjust the peak and the background to minimize the chi-square of the fitting on each spectra. Fig. 2 shows the spectrum of La.

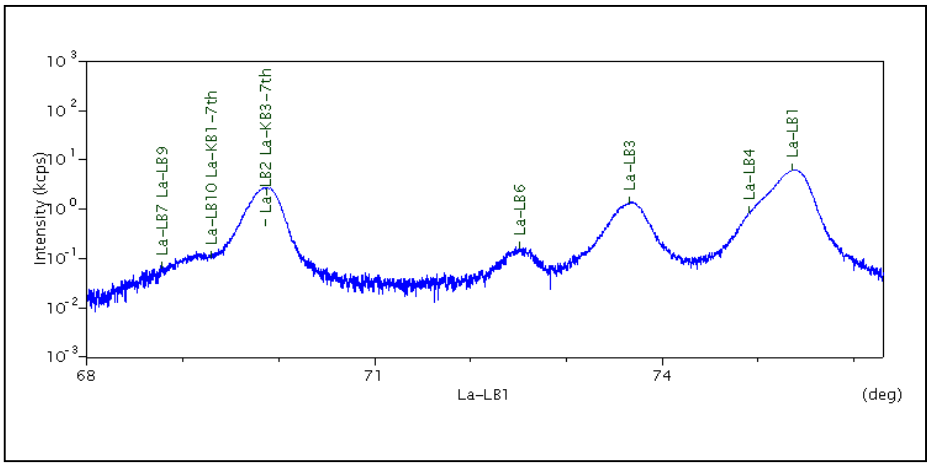

Fig. 2. Measured spectrum of La *Lβ* X-rays.

3. Results and Discussion

When a sample is irradiated with high energy X-ray photons it will emit characteristic X-ray lines whose energy depends on the atomic number of the element of the sample material. If a sample consists of a chemical compound or mixture, its fluorescence spectrum will also be complex. Because the inner electron shells between which the X-ray transitions occur are not involved in the chemical bonds, the characteristic lines are largely independent of the chemical bonds of the element. This means that the X-ray fluorescence spectra of a chemical compound are, in a first approximation, a superposition of the spectra of its components. Qualitative analysis involves identifying atoms present in a specimen by associating observed characteristic lines with their atoms. Quantitative analysis involves determining the amount of each atom present in the specimen from the intensity of measured characteristic X-ray lines.

The measured chemical shifts (ΔE) in *L* X-ray emission lines for La and Ce compounds in different chemical forms are presented in Table 1. As can be seen from Table 1, when all *L* transitions based on, it has been determined that the $La_2(CO_3)_3.8H_2O$ in the orthorhombic structure is symmetrical but the $La_2(C_2O_4)_3.10H_2O$ compound in the cubic structure is in the asymmetric form. The two compounds $LaCl_3$ and La_2O_3in the hexagonal structure have 9 and 7 coordination numbers, respectively.

Cerium is an element of interest because it has a variable electronic structure. At 4f level, the electrons in the outer layer or valence layer are very close to each other; so that the electronic configuration can be changed with very little energy (pressure or temperature change). Cerium has three levels of oxidation (+2, +3 and +4).

As can be seen from Table 1, the *Lα* and *Lβ* peaks gain a more symmetrical structure with increasing oxidation number. Thus, compounds CeH_4, Ce_2O_4, Ce $(SO_4)_2 \cdot 4H_2O$ at the +4-valence level are symmetric while compounds $Ce_2(CO_3)_3 \cdot 5H_2O$, CeF_3, $Ce_2(SO_4)_3 \cdot 8H_2O$ at the + 3 oxidation level are more asymmetric.

In general, we know that the *K*-emission lines of the 3d elements have an asymmetric structure. In this study, we also see that the *L*-layer emission lines of the compounds of the lanthanide group are asymmetric. The FWHM ratio values of the *Lα*, *Lβ* and *Lγ* emission lines of the dysprosium compounds are in the range of 0.925 and 1.319. Among all the compounds, Dy $(NO_3)_3$ has a maximum FWHM ratio value of $L_{\gamma 3}$. When FWHM values are compared, it was found a change in the range of 0.708 to 1.646 for Lantan and 0,460 to 1,663 for Cerium.

When we compare the chemical structure of all the elements compared to the pure state, we can clearly see that the peak center point corresponding to 9/10 of the line maximum intensity has changed. Parameters such as the number of 3d electrons, crystal structure also affect this change (chemical shift). The chemical shift values increase with increasing oxidation number and also in the Cerium compounds with the same number of oxides, the shifts in different amounts are observed. A number of reasons for this are: Electronegativity is the distribution of ligands around the central atom and the atoms from which the ligands are formed. With increasing oxidation number emission lines are increasingly narrow and FWHM values are gradually reduced as it relates.

Table 1. Energy shifts (ΔE), asymmetry indices (AI) and ratio of full with at half maximum (FWHM) values of *L* emission lines in Lanthanum compounds.

Element	Emission Lines	Δ*E*(eV)	AI	$FWHM_{compound}/FWHM_{pure}$
La	$L\alpha_1$	0	1,027	1
	$L\alpha_2$	0	1,061	1
	$L\beta_1$	0	1,027	1
	$L\beta_2$	0	1,000	1
	$L\beta_3$	0	0,977	1
	$L\beta_4$	0	0,944	1
	$L\beta_6$	0	0,965	1
	$L\gamma_1$	0	1,000	1
	$L\gamma_2$	0	1,017	1
	$L\gamma_3$	0	1,007	1
	$L\alpha_1$	0	1,000	0,990
	$L\alpha_2$	+0, 01	1,021	0,941

	$L\beta_1$	0	1,054	1,024
	$L\beta_2$	-0, 92	1,031	0,957
$La_2(CO_3)_3.8H_2O$	$L\beta_3$	-0,01	0,966	0,994
	$L\beta_4$	+0,05	0,976	1,161
	$L\beta_6$	-0,05	0,985	1,086
	$L\gamma_1$	-0,10	0,980	0,901
	$L\gamma_2$	-0,05	1,041	1,225
	$L\gamma_3$	-0,39	1,027	1,020
	$L\alpha_1$	-0,01	0,973	0,967
	$L\alpha_2$	+0,06	0,955	1,458
	$L\beta_1$	+0,07	1,000	1,116
	$L\beta_2$	-0,42	1,010	1,406
	$L\beta_3$	-0,04	1,000	1,092
$La_2(C_2O_4)_3.10H_2O$	$L\beta_4$	+0,30	1,000	1,032
	$L\beta_6$	-0,03	0,974	1,010
	$L\gamma_1$	-0,01	1,000	1,004
	$L\gamma_2$	-0,05	1,014	1,148
	$L\gamma_3$	-0,23	1,042	0,812
	$L\alpha_1$	+0,01	1,014	0,964
	$L\alpha_2$	+0,06	0,988	1
	$L\beta_1$	-0,06	1,014	1,646
	$L\beta_2$	-0,11	1,000	1,004
	$L\beta_3$	+0,07	1,011	1,032
$LaCl_3$	$L\beta_4$	-0,19	0,981	1,480
	$L\beta_6$	+0,05	1,000	1,043
	$L\gamma_1$	+0,01	1,000	0,937
	$L\gamma_2$	+0,10	0,975	0,992
	$L\gamma_3$	+0,17	1,000	1,111

	$L\alpha_1$	+0,01	1,000	1,020
	$L\alpha_2$	-0,01	1,000	0,931
	$L\beta_1$	+0,04	0,976	1,102
	$L\beta_2$	-0,42	0,990	1,442
	$L\beta_3$	+0,06	0,989	1,032
	$L\beta_4$	+0,25	0,977	1,197
La_2O_3	$L\beta_6$	-0,08	1,011	1,217
	$L\gamma_1$	+0,01	1,009	1,059
	$L\gamma_2$	-0,06	1,016	1,049
	$L\gamma_3$	-0,08	1,039	0,883
	$L\alpha_1$	+0,01	1,013	0,997
	$L\alpha_2$	+0,06	1,020	1,015
	$L\beta_1$	-0,02	1,014	1,014
	$L\beta_2$	-0,43	1,010	1,431
$La_2(SO_4)_3.9H_2O$	$L\beta_3$	-0,08	0,990	1,107
	$L\beta_4$	-0,05	1,000	1,165
	$L\beta_6$	-0,02	0,986	0,911
	$L\gamma_1$	-0,04	0,991	1,027
	$L\gamma_2$	-0,09	1,000	1,045
	$L\gamma_3$	-0,13	0,992	0,826
	$L\alpha_1$	+0,03	1,038	1,046
	$L\alpha_2$	-0,10	0,863	0,951
	$L\beta_1$	0	1,013	1,068
	$L\beta_2$	-0,55	1,015	0,967
LaF_3	$L\beta_3$	-0,03	1,012	0,965
	$L\beta_4$	+0,08	1,011	1,355
	$L\beta_6$	0	1,013	1,046
	$L\gamma_1$	-0,06	1,000	1,090

	$L\gamma_2$	-0,18	1,000	1,357
	$L\gamma_3$	-0,67	0,990	0,708

Table 2. Energy shifts (ΔE), asymmetry indices and ratio of full with at half maximum (FWHM) values of *L* emission lines in Cerium compounds.

Element	**Emission Lines**	**Δ*E*(eV)**	**AI**	**$FWHM_{compound}/FWHM_{pure}$**
Ce	*Lα1*	0	1,000	1
	Lα2	0	1,000	1
	Lβ1	0	1,012	1
	Lβ2	0	1,011	1
	Lβ3	0	1,019	1
	Lβ4	0	0,982	1
	Lβ6	0	1,024	1
	Lγ1	0	1,032	1
	Lγ2	0	0,988	1
	Lγ3	0	0,981	1
CeF_3	$L\alpha_1$	+0,05	1,023	1,138
	$L\alpha_2$	-0,21	1,000	1,039
	$L\beta_1$	-0,07	1,000	0,988
	$L\beta_2$	+0,10	1,000	1,069
	$L\beta_3$	+0,10	1,017	1,159
	$L\beta_4$	-0,13	1,024	1,543
	$L\beta_6$	+0,01	0,979	1,142
	$L\gamma_1$	0	1,033	0,954
	$L\gamma_2$	+0,75	0,970	0,645
	$L\gamma_3$	-9,59	1,027	0,959
	$L\alpha_1$	+0,02	0,989	1,080
	$L\alpha_2$	-0,15	0,963	0,795
	$L\beta_1$	-0,01	1,000	1,027

	$L\beta_2$	+0,17	1,000	1,169
$Ce_2(SO_4)_3 \cdot 8H_2O$	$L\beta_3$	+0,15	1,014	1,419
	$L\beta_4$	+0,05	1,014	1,362
	$L\beta_6$	+0,13	0,993	1,663
	$L\gamma_1$	+0,49	1,007	1,526
	$L\gamma_2$	+0,64	0,986	0,583
	$L\gamma_3$	-9,38	0,750	0,662
	$L\alpha_1$	0	1,000	1,103
	$L\alpha_2$	-0,13	1,047	0,680
	$L\beta_1$	-0,18	0,987	0,887
	$L\beta_2$	-0,34	1,014	0,803
CeH_4	$L\beta_3$	+0,06	1,000	1,137
	$L\beta_4$	-0,47	1,012	1,466
	$L\beta_6$	-0,01	1,041	1,243
	$L\gamma_1$	+0,18	1,049	1,088
	$L\gamma_2$	+0,91	0,991	0,460
	$L\gamma_3$	-8,79	1,013	1,003
	$L\alpha_1$	-0,02	1,013	1,032
	$L\alpha_2$	-0,09	0,982	0,846
	$L\beta_1$	-0,30	1,016	0,761
	$L\beta_2$	+0,09	0,990	1,117
	$L\beta_3$	+0,05	0,990	0,931
	$L\beta_4$	-0,74	1	1,615
	$L\beta_6$	+0,07	1,013	0,941
Ce_2O_4	$L\gamma_1$	-0,03	0,970	1,021
	$L\gamma_2$	+0,91	0,986	0,559
	$L\gamma_3$	-9,14	1,017	1,092
	$L\alpha_1$	0	0,977	1,145

	$L\alpha_2$	-0,23	1,068	0,927
	$L\beta_1$	-0,06	1,000	0,994
	$L\beta_2$	+0,12	1,000	1,074
$Ce(SO_4)_2 \cdot 4H_2O$	$L\beta_3$	0	0,982	1,059
	$L\beta_4$	-0,12	1,028	1,339
	$L\beta_6$	+0,14	1,026	0,935
	$L\gamma_1$	+0,14	0,990	1,010
	$L\gamma_2$	+0,88	1,000	0,537
	$L\gamma_3$	-9,15	1,006	1,076
	$L\alpha_1$	+0,01	0,976	1,071
	$L\alpha_2$	-0,15	0,964	0,838
	$L\beta_1$	-0,09	1,000	0,952
	$L\beta_2$	-0,10	1,012	0,943
$Ce_2(CO_3)_3 \cdot 5H_2O$	$L\beta_3$	+0,01	1,000	0,912
	$L\beta_4$	-0,22	1,000	1,398
	$L\beta_6$	+0,09	1,014	0,870
	$L\gamma_1$	+0,08	1,010	0,985
	$L\gamma_2$	+0,78	1,020	0,595
	$L\gamma_3$	-9,39	1,071	0,909

The L_β and L_γ lines are the resultant transitions of the valence electrons and these lines change with the chemical structure change. The energy shifts in the $L_{\beta 6}$ line given in Table 1 are greater than the shifts in the other L_β line. Also, from Table 2 we can see that the cerium compounds have an asymmetric structure when compared to the others and that the shear values of these compounds are larger. Compounds where the asymmetry index is large, the peak expands in the low energy region.

4. Conclusion

Based on our assessments of the results obtained using WDXRF spectrometry with good separation power, we can say that we observed significant changes in the peak shapes of the lanthanide group compounds (asymmetry index, full width at half maximum, energy shift). An answer has been sought to ask what or what might cause these exchanges. In different compositions, the compounds of the elements of many lanthanide groups were investigated. The results are interpreted in terms of number of oxidations, number of coordination, changes in crystal and molecular structures. In addition, this study has been one of the most detailed studies made in the literature in order to determine whether there

is a chemical effect on the *L*-layer transition. By taking advantage of the characteristic *L* X-ray spectra, it is planned to continue our studies in order to show whether there is a similar effect on the relative intensity values and the satalit lines.

5. References

1- P. Glatzel,U. Bergmann, *High resolution 1s core hole X-ray spectroscopy in 3d transition metal complexes-electronic and structural information*, Coordination Chemistry Reviews, 2005, 249, 65-95.

2- J.H. Guo, S.M. Butorin, N. Wassdahl, P. Skytt, J. Nordgren and Y. Ma, *Electronic structure of La2−xSrxCuO4 studied by soft-x-ray-fluorescence spectroscopy with tunable excitation*, Phys. Rev. B, 1994, 49, 1376.

3- S.M. Butorin, D.C. Mancini, J.H. Guo, N. Wassdahl, J. Nordgren, M. Nakazawa, S. Tanaka, T. Uozumi, A. Kotani, Y. Ma, K. E. Myano, B.A. Karlin and D.K. Shuh, *Resonant X-Ray Fluorescence Spectroscopy of Correlated Systems: A Probe of Charge-Transfer Excitations*, Phys. Rev. Lett., 1996, 77, 574.

4- T.Yoshimuraa, Y. Tamenori, A. Suzuki, R. Nakashima, N. Iwasaki, H. Hasegawae, H. Kawahataa, *Element profile and chemical environment of sulfur in a giant clam shell: Insights from μ-XRF and X-ray absorption near-edge structure*, Chemical Geology, 2013, 352, 170-175.

5- D.B. Hunter, P.M. Bertsch, K.M. Kemner and S.B. Clark, *Distribution and Chemical Speciation of Metals and Metalloids in Biota Collected from Contaminated Environments by Spatially Resolved XRF, XANES, and EXAFS,* Proceedings of the 9th International Conference on X-Ray Absorption Fine Structure, J. Phys. IV, France 1997, C2-767-771.

6- E. Boydaş, E. Orhan, M.G. Boydaş, E. Cömert, *Chemical shifts of Ka and Kb1,3 X-ray emission spectra for oxygen compounds of Ti, Cr, Fe, Co, Cu with WDXRF*, Procedia - Social and Behavioral Sciences 195 (2015) 1757 –1761.

7- S. Porikli, D. Demir and Y. Kurucu, *Variation of Kβ/Kα X-ray intensity ratio and lineshape with the effects of external magnetic field and chemical combination*, 2008, Eur. Phys. J. D 47, 315–323.

8- S. Nishibu, S. Yonezawa, M. Takashima, J. Fluorine Chem. 2005, 126, 1048.

9- H.S. Kainth, R.Singh, J.S. Shahi, T. Singh, *Study of chemical shift in Ll and Lη X-ray emission lines in different chemical forms of 48Cd and 50Sn compounds using WDXRF technique*, X-Ray Spectrometry, 2018, 47(2), 116-126.

10- S. Raj, H.C. Padhi, M. Polasik, *Influence of chemical effect on the Kβ-to-Kα x-ray intensity ratios of Cr, Mn and Co in CrSe, MnSe, MnS and CoS*, Nuclear Instruments and Methods in Physics Research Section B, 160(4), 443-448.

11- S. Porikli, Y. Kurucu, *Effect of an External Magnetic Field on the Kα and Kβ X-Ray Emission Lines of the 3d Transition Metals*, Instrumentation Science&Technology, 2008, 36(4), 341-354.

12- H. Baltas, B. Ertugral, C. Kantar, S. Sasmaz, E. Yılmaz and U. Cevik, *Kβ/Kα X-Ray Intensity Ratios for Co, Ni, Cu, and Zn in Phthalocyanines Complexes*, Acta Physica Polonica, 2011, 119(6), 764-768.